REPORT DOCUMENTATION PAGE

Form Approved
OMB No. 0704-0188

AD-A244 883

2. REPORT DATE	3. REPORT TYPE AND DATES COVERED
December 1991	professional paper

4. TITLE AND SUBTITLE

MULTIPLY-CONSTRAINED MVDR MATCHED FIELD PROCESSING WITH A-POSTERIORI CONSTRAINTS FOR ENHANCED ROBUSTNESS TO MISMATCH

5. FUNDING NUMBERS

PR: SW17
PE: 0602314N
WU: DN308291

6. AUTHOR(S)

S. I. Chow, M. D. Zoltowski, and G. M. Kautz

7. PERFORMING ORGANIZATION NAME(S) AND ADDRESS(ES)

Naval Ocean Systems Center
San Diego, CA 92152–5000

8. PERFORMING ORGANIZATION REPORT NUMBER

9. SPONSORING/MONITORING AGENCY NAME(S) AND ADDRESS(ES)

Office of Naval Technology
Office of Chief of Naval Research
Arlington, VA 22217–5000

10. SPONSORING/MONITORING AGENCY REPORT NUMBER

11. SUPPLEMENTARY NOTES

12a. DISTRIBUTION/AVAILABILITY STATEMENT

Approved for public release; distribution is unlimited.

12b. DISTRIBUTION CODE

13. ABSTRACT *(Maximum 200 words)*

It has been proposed that source localization in passive sonar be accomplished via some form of Matched Field Processing (MFP). Full-coherent, Minimum Variance Distortionless Response (MVDR) MFP assumes complete and perfect characterization of the underwater multipath propagation channel and is known to be extremely sensitive to mismatch between model parameters and actual environmental parameters. We present a minimax, multi-rank signal variation of MVDR MFP referred to as Semi-coherent MVDR MFP. Simulation results are presented demonstrating Semi-coherent MVDR MFP to be both relatively robust to mismatch, with respect to relative amplitudes and phases amongst multipath arrivals, and comparable in performance to Full-coherent MVDR MFP under no mismatch conditions.

Published in *Conference Record of the 25th Asilomer Conference on Signals, Systems, and Computers*, November, 1991.

14. SUBJECT TERMS

acoustic detection
arrays

15. NUMBER OF PAGES

16. PRICE CODE

17. SECURITY CLASSIFICATION OF REPORT	18. SECURITY CLASSIFICATION OF THIS PAGE	19. SECURITY CLASSIFICATION OF ABSTRACT	20. LIMITATION OF ABSTRACT
UNCLASSIFIED	UNCLASSIFIED	UNCLASSIFIED	SAME AS REPORT

21a. NAME OF RESPONSIBLE INDIVIDUAL	21b. TELEPHONE *(Include Area Code)*	21c. OFFICE SYMBOL
S. I. Chow	(619) 553-2541	Code 761

Accession For	
NTIS GRA&I	☑
DTIC TAB	☐
Unannounced	☐
Justification	
By	
Distribution/	
Availability Codes	
Dist	Avail and/or Special
A-1	

Multiply-Constrained MVDR Matched Field Processing with A-Posteriori Constraints for Enhanced Robustness to Mismatch[†]

Michael D. Zoltowski[*], Gregory M. Kautz[*], and S. I. Chou[**]

[*]School of Electrical Engineering, Purdue University, West Lafayette, IN 47907
[**]Naval Ocean Systems Center, San Diego, CA 92152-5000

Abstract

It has been proposed that source localization in passive sonar be accomplished via some form of Matched Field Processing (MFP). Full-coherent, Minimum Variance Distortionless Response (MVDR) MFP assumes complete and perfect characterization of the underwater multipath propagation channel and is known to be extremely sensitive to mismatch between model parameters and actual environmental parameters. We present a minimax, multi-rank signal variation of MVDR MFP referred to as Semi-coherent MVDR MFP. Simulation results are presented demonstrating Semi-coherent MVDR MFP to be both relatively robust to mismatch, with respect to relative amplitudes and phases amongst multipath arrivals, and comparable in performance to Full-coherent MVDR MFP under no mismatch conditions.

1. Introduction

Consider a candidate source location (i. e., a point on a search grid) designated by the position vector $\vec{r} = (R, \theta, z)$ with respect to a cylindrical coordinate system centered at some reference point in the array. Through acoustic ray tracing, we determine the respective arrival angle of each ray path between the candidate source location and some reference point in the array. Let L denote the number of dominant ray paths based on ray tracing prediction. In the case of a linear array, we denote the Lx1 vector composed of the L conical arrival angles as $\underline{\theta}$, i. e., $\underline{\theta} = (\theta_1, \theta_2, \cdots, \theta_L)$, where θ_i is the conical arrival angle associated with the i-th ray path, i=1,...,L. With further modeling, we could determine the relative amplitudes and phases amongst the L multipath arrivals. However, the relative phases of the multipath arrivals can change dramatically with small changes in the ocean parameters, a change in the ocean depth, for example [1]. As a step towards developing a robust procedure, we will not assume knowledge of the relative amplitudes and phases of the multipath arrivals for any source location. Rather, we will only assume knowledge of θ_i and the corresponding steering vector, denoted $\mathbf{a}_i$, i=1,...,L, for each of the L dominant ray paths.

2. Semi–coherent MVDR MFP

Semi-coherent MVDR MFP is developed as a minimax approach to the source localization problem. Let N denote the number of sensors comprising the array. An Nx1 weight vector is constructed to *minimize* the average power of the corresponding beamformer output under a constraint on the gain and phase response in each of the L multipath arrival directions. The gain and phase response pairs, one for each multipath arrival direction, are jointly determined so as to *maximize* the SNR of the beamformer output. The minimization stage may be mathematically posed as the following constrained optimization problem:

$$\underset{\mathbf{w}(\vec{r})}{\text{Minimize}}\ \mathbf{w}^H(\vec{r})\mathbf{R}_{xx}\mathbf{w}(\vec{r}) \qquad (2.1)$$

$$\text{subject to:}\quad \mathbf{A}^H(\underline{\theta})\mathbf{w}(\vec{r}) = \boldsymbol{\delta}$$

where $\boldsymbol{\delta} = [\delta_1, \delta_2, \cdots, \delta_L]^T$, an Lx1 vector, and $\mathbf{A}(\underline{\theta}) = [\mathbf{a}_1, \mathbf{a}_2, \cdots, \mathbf{a}_L]$, an NxL matrix. The magnitude and phase of δ_i represent the gain and phase response, respectively, in the i-th multipath arrival direction, i=1,...,L. Assuming $L < N$, $\mathbf{A}^H(\underline{\theta})\mathbf{w}(\vec{r}) = \boldsymbol{\delta}$ represents an underdetermined system of equations. The solution to (2.1) is simply the minimum norm solution to $\mathbf{A}^H(\underline{\theta})\mathbf{w}(\vec{r}) = \boldsymbol{\delta}$ in a Hilbert space with inner product $\langle \mathbf{x}, \mathbf{y} \rangle = \mathbf{y}^H\mathbf{R}_{xx}\mathbf{x}$:

$$\mathbf{w}(\vec{r}) = \mathbf{R}_{xx}^{-1}\mathbf{A}(\underline{\theta})\left[\mathbf{A}^H(\underline{\theta})\mathbf{R}_{xx}^{-1}\mathbf{A}(\underline{\theta})\right]^{-1}\boldsymbol{\delta} \qquad (2.2)$$

Motivated by the work of Krolik, Lynch, and Swingler in developing "Incoherent" MVDR MFP [1][1], we define the

[†]This work was supported by the Naval Ocean Systems Center (NOSC) under contract no. N66001-87-D-0136 with Office of Naval Technology (ONT) funding.

[1] James Wilson of Neptune Sciences, Inc. is acknowledged for referring the third author to ref. [1].

To appear in Conference Record of the 25th Asilomar Conference on Signals, Systems and Computers, Nov. 4-6, 1991, Pacific Grove, CA.

value of the Semi-coherent MVDR MFP ambiguity surface at a point $\vec{r}$ for a given beam response constraint vector δ, denoted $S_{Semi}(\vec{r}\,;\delta)$, to be the SNR of the beamformer output obtained with $w(\vec{r})$ in (2.2). Actually, since we don't have access to signal-only data, we will define it to be the signal plus noise to noise ratio.

For the sake of simplicity, we will assume the noise to be spatially white with the power of the noise at each sensor element equal to σ_n^2. In this case, the output signal plus noise to noise ratio, (S+N)/N, is proportional to $w^H(\vec{r})R_{xx}w(\vec{r})\,/\,w^H(\vec{r})w(\vec{r})$. With $w(\vec{r})$ given by (2.2), $S_{Semi}(\vec{r}\,;\delta)$ may be expressed, after some manipulation, as

$$S_{Semi}(\vec{r}\,;\delta) = \frac{\delta^H M_1^{-1} M_1 M_1^{-1}\delta}{\delta^H M_1^{-1} M_2 M_1^{-1}\delta} \qquad (2.3)$$

where M_1 and M_2 are defined as

$$M_1 = A^H(\underline{\theta})R_{xx}^{-1}A(\underline{\theta}) \qquad (2.4a)$$

$$M_2 = A^H(\underline{\theta})R_{xx}^{-2}A(\underline{\theta}) \qquad (2.4b)$$

Note that in accordance with the minimax principle underlying Semi-coherent MVDR MFP espoused previously, δ is taken to be that value which maximizes $S_{Semi}(\vec{r}\,;\delta)$. Since $S_{Semi}(\vec{r}\,;\delta)/\sigma_n^2 = (S+N)/N = S/N + 1$, this is equivalent to maximizing the beamformer output SNR. Defining $\beta = M_1^{-1}\delta$, we may alternatively define $S_{Semi}(\vec{r})$ as

$$S_{Semi}(\vec{r}) = \underset{\beta}{\text{Maximum}}\ \frac{\beta^H A^H(\underline{\theta})R_{xx}^{-1}A(\underline{\theta})\beta}{\beta^H A^H(\underline{\theta})R_{xx}^{-2}A(\underline{\theta})\beta} \qquad (2.5)$$

The maximizing β is the generalized eigenvector associated with the largest generalized eigenvalue of the LxL matrix pencil $\{A^H(\underline{\theta})R_{xx}^{-1}A(\underline{\theta})\,,\,A^H(\underline{\theta})R_{xx}^{-2}A(\underline{\theta})\}$. In turn, $S_{Semi}(\vec{r})$ is the largest generalized eigenvalue of $\{A^H(\underline{\theta})R_{xx}^{-1}A(\underline{\theta})\,,\,A^H(\underline{\theta})R_{xx}^{-2}A(\underline{\theta})\}$.

3. Comparison of Semi–coherent MVDR MFP With Full–coherent MVDR MFP

Let $c(\vec{r})$ denote the Lx1 vector composed of the relative complex amplitudes of the L multipath arrivals for a candidate source location $\vec{r}$; $c(\vec{r})$ is normalized such that $c^H(\vec{r})c(\vec{r}) = 1$. The Full-coherent MVDR MFP beamformer for a candidate search location $\vec{r}$ is the solution to the single constraint MVDR problem

$$\underset{w(\vec{r})}{\text{Minimize}}\ E\{|w^H(\vec{r})x(n)|^2\} = w^H(\vec{r})R_{xx}w(\vec{r})$$

$$\text{subject to:}\quad w^H(\vec{r})\,\{A(\underline{\theta})c(\vec{r})\} = 1 \qquad (3.1)$$

Thus, in addition to knowledge of the arrival angle and corresponding steering vector for each ray path, Full-coherent MVDR MFP also assumes knowledge of the relative amplitudes and phases amongst the L ray paths. In addition, Full-coherent MVDR MFP assumes the multipath arrivals to be 100% correlated. In contrast, proper operation of Semi-coherent MVDR MFP is not premised on such -- the multipath arrivals corresponding to the same source may be partially correlated or 100% correlated.

Similar to the solution to (2.1), the solution to (3.1) is the minimum norm solution to the constraint equation with the norm induced by the inner product $\langle x\,,\,y\rangle = y^H R_{xx} x$.

$$w(\vec{r}) = \frac{1}{c^H(\vec{r})A^H(\underline{\theta})R_{xx}^{-1}A(\underline{\theta})c(\vec{r})}\,R_{xx}^{-1}A(\underline{\theta})c(\vec{r}) \qquad (3.2)$$

Similar to Semi-coherent MVDR MFP, we define the value of the Full-coherent MVDR MFP ambiguity surface at a point $\vec{r}$, denoted $S_{Full}(\vec{r})$, as $w^H(\vec{r})R_{xx}w(\vec{r})\,/\,w^H(\vec{r})w(\vec{r})$ with $w(\vec{r})$ given by (3.2). Again, this is proportional to the output (S+N)/N with the set of weights described by (3.2). Substituting (3.2), we obtain, after some algebraic manipulation,

$$S_{Full}(\vec{r}) = \frac{c^H(\vec{r})A^H(\underline{\theta})R_{xx}^{-1}A(\underline{\theta})c(\vec{r})}{c^H(\vec{r})A^H(\underline{\theta})R_{xx}^{-2}A(\underline{\theta})c(\vec{r})} \qquad (3.3)$$

Note that the expression for $S_{Full}(\vec{r})$ is very similar to the expression for the objective function in the defining expression for $S_{Semi}(\vec{r})$ in (2.5).

We now examine the performance of Semi-coherent MVDR MFP in the case of a single source at $\vec{r}_s$ and no interferers. We will assume the L multipath arrivals to be 100% correlated. In this case, the covariance matrix has the asymptotic form

$$R_{xx} = \sigma_s^2 A(\underline{\theta}_s)c(\vec{r}_s)c^H(\vec{r}_s)A^H(\underline{\theta}_s) + \sigma_n^2 I \qquad (3.4)$$

where σ_s^2 is the sum of the square-amplitude of each of the L multipath arrivals. We want to examine the value of $S_{Semi}(\vec{r})$ at $\vec{r} = \vec{r}_s$ when R_{xx} has the asymptotic form in (3.4). In our analysis we will need expressions for R_{xx}^{-1} and R_{xx}^{-2}. It is easy to verify that

$$R_{xx}^{-1} = \frac{1}{\lambda_1}\frac{1}{\alpha_s}A(\underline{\theta}_s)c(\vec{r}_s)c^H(\vec{r}_s)A^H(\underline{\theta}_s) + \frac{1}{\sigma_n^2}P^{\perp} \qquad (3.5)$$

where

$$\alpha_s = c^H(\vec{r}_s)A^H(\underline{\theta}_s)A(\underline{\theta}_s)c(\vec{r}_s) = \|A(\underline{\theta}_s)c(\vec{r}_s)\|^2 \quad (3.6a)$$

$$\lambda_1 = \sigma_s^2\alpha_s + \sigma_n^2 \quad (3.6b)$$

and $\mathbf{P}^{\perp}$ is the projection operator onto the orthogonal complement of the 1-D space spanned by $A(\underline{\theta}_s)c(\vec{r}_s)$ such that

$$\mathbf{P}^{\perp}A(\underline{\theta}_s)c(\vec{r}_s) = 0 \quad (3.7a)$$

$$c^H(\vec{r}_s)A^H(\underline{\theta}_s)\mathbf{P}^{\perp}A(\underline{\theta}_s)c(\vec{r}_s) = 0 \quad (3.7b)$$

Squaring the expression in (3.5), we obtain, after some algebraic manipulation, a similar expression for $\mathbf{R}_{xx}^{-2}$:

$$\mathbf{R}_{xx}^{-2} = \frac{1}{\lambda_1^2}\frac{1}{\alpha_s}A(\underline{\theta}_s)c(\vec{r}_s)c^H(\vec{r}_s)A^H(\underline{\theta}_s) + \frac{1}{\sigma_n^4}\mathbf{P}^{\perp} \quad (3.8)$$

$S_{Semi}(\vec{r}_s)$ is the largest generalized eigenvalue of $\{A^H(\underline{\theta}_s)\mathbf{R}_{xx}^{-1}A(\underline{\theta}_s)\ ,\ A^H(\underline{\theta}_s)\mathbf{R}_{xx}^{-2}A(\underline{\theta}_s)\}$. To evaluate this, we first observe (3.9)

$$\{A^H(\underline{\theta}_s)\mathbf{R}_{xx}^{-1}A(\underline{\theta}_s)\}\ c(\vec{r}_s) = \lambda_1\ \{A^H(\underline{\theta}_s)\mathbf{R}_{xx}^{-2}A(\underline{\theta}_s)\}\ c(\vec{r}_s)$$

where we have employed the asymptotic forms of $\mathbf{R}_{xx}^{-1}$ and $\mathbf{R}_{xx}^{-2}$ in (3.5) and (3.8), respectively, and invoked the property in (3.7). (3.9) dictates that $c(\vec{r}_s)$ is a generalized eigenvector of $\{A^H(\underline{\theta}_s)\mathbf{R}_{xx}^{-1}A(\underline{\theta}_s)\ ,\ A^H(\underline{\theta}_s)\mathbf{R}_{xx}^{-2}A(\underline{\theta}_s)\}$ associated with the generalized eigenvalue λ_1, where λ_1 is defined in (3.6b). We now show that the remaining L-1 generalized eigenvalues are equal to the noise power σ_n^2.

Let $\mathbf{e}_i$, i=1,...,L, denote the generalized eigenvectors of $\{A^H(\underline{\theta}_s)\mathbf{R}_{xx}^{-1}A(\underline{\theta}_s)\ ,\ A^H(\underline{\theta}_s)\mathbf{R}_{xx}^{-2}A(\underline{\theta}_s)\}$. Since $A^H(\underline{\theta}_s)\mathbf{R}_{xx}^{-1}A(\underline{\theta}_s)$ and $A^H(\underline{\theta}_s)\mathbf{R}_{xx}^{-2}A(\underline{\theta}_s)$ are both Hermitian, the generalized eigenvectors are orthogonal in the metric $A^H(\underline{\theta}_s)\mathbf{R}_{xx}^{-2}A(\underline{\theta}_s)$, i. e., $\mathbf{e}_i^H A^H(\underline{\theta}_s)\mathbf{R}_{xx}^{-2}A(\underline{\theta}_s)\mathbf{e}_j = 0$ for $i \neq j$. Since $c(\vec{r}_s)$ is a generalized eigenvector, it follows that

$$c^H(\vec{r}_s)A^H(\underline{\theta}_s)\mathbf{R}_{xx}^{-2}A(\underline{\theta}_s)\,\mathbf{e}_j = 0 \quad j=2,...,L \quad (3.10)$$

Substituting the expression for $\mathbf{R}_{xx}^{-2}$ in (3.8) above and exploiting the property in (3.7) yields the following simplification of (3.10):

$$c^H(\vec{r}_s)A^H(\underline{\theta}_s)A(\theta_j)\,\mathbf{e}_j = 0 \quad j=2,...,L \quad (3.11)$$

Invoking the asymptotic forms of $\mathbf{R}_{xx}^{-1}$ and $\mathbf{R}_{xx}^{-2}$ in (3.5) and (3.8), respectively, and the properties in (3.6) and (3.11), we find, after some manipulation, that for j=2,...,L,

$$\{A^H(\underline{\theta}_s)\mathbf{R}_{xx}^{-1}A(\underline{\theta}_s)\}\ \mathbf{e}_j = \sigma_n^2\{A^H(\underline{\theta}_s)\mathbf{R}_{xx}^{-2}A(\underline{\theta}_s)\}\ \mathbf{e}_j \quad (3.12)$$

Thus, since $\sigma_s^2\alpha_s + \sigma_n^2 > \sigma_n^2$, the largest generalized eigenvalue of $\{A^H(\underline{\theta}_s)\mathbf{R}_{xx}^{-1}A(\underline{\theta}_s)\ ,\ A^H(\underline{\theta}_s)\mathbf{R}_{xx}^{-2}A(\underline{\theta}_s)\}$, and hence the value of $S_{Semi}(\vec{r}_s)$, is $\lambda_1 = \sigma_s^2\alpha_s + \sigma_n^2$, where α_s is defined in (3.6a). In addition, the corresponding generalized eigenvector, and hence the value of β which maximizes the objective function in (2.5), is $c(\vec{r}_s)$.

It follows from previous observations that the signal plus noise to noise ratio, (S+N)/N, achieved with both Semi-coherent MVDR MFP and Full-coherent MVDR MFP at the point $\vec{r}_s$ is $S_{Semi}(\vec{r}_s)/\sigma_n^2$ and $S_{Full}(\vec{r}_s)/\sigma_n^2$, respectively, and that these are equal if $\beta = c(\vec{r}_s)$ in (2.5). The previous development demonstrated that in the asymptotic case $\beta = c(\vec{r}_s)$ in the case of a single source, assuming "adequate" SNR, and that $S_{Semi}(\vec{r}_s) = \sigma_s^2\alpha_s + \sigma_n^2$. Since (S+N)/N = S/N + 1, it follows that the asymptotic SNR achieved with both Semi-coherent MVDR MFP and Full-coherent MVDR MFP at the point $\vec{r}_s$ is $(\sigma_s^2\alpha_s + \sigma_n^2)/\sigma_n^2 - 1$ such that

$$SNR_{Full}(\vec{r}_s) = SNR_{Semi}(\vec{r}_s) = \frac{\sigma_s^2}{\sigma_n^2}\|A(\underline{\theta}_s)c(\vec{r}_s)\|^2 \quad (3.13)$$

where $\|x\|$ denotes the 2-norm of the vector x. Again, the fact that Semi-coherent MVDR MFP yielded the same output SNR at the true source location as that achieved with Full-coherent MVDR MFP hinged on β being equal to the vector of normalized complex amplitudes $c(\vec{r}_s)$. We only proved this to be true in the asymptotic case with a single source. In general, β will only be approximately equal to $c(\vec{r}_s)$. This is the reason we refer to the method as "Semi-coherent" in contrast to Full-coherent.

4. Incoherent MVDR MFP

Krolik, Lynch, and Swingler [1] also take a multi-rank signal approach to the source localization problem. For each point on the search grid, they computing a multiply-constrained MVDR beamforming weight vector according to (2.2) with δ equal to **1**, a vector composed of all ones. The value of the "Incoherent" MVDR MFP ambiguity surface at $\vec{r}$ may be computed according to (2.3) with $\delta = \mathbf{1}$, i. e., $S_{Incoh}(\vec{r}) = S_{Semi}(\vec{r}\ ;\mathbf{1})$.

5. Simulations

A very simple ocean model was employed in the simulations to illustrate fundamental aspects of each of the three versions of MVDR MFP without getting lost in modeling issues. In this model, an iso-velocity ocean is assumed with a sound speed of 1500 m/s and a nominal

depth of 4500 m. The receiving array is vertically oriented and composed of 30 sensors equi-spaced by a half-wavelength (7.5 m) at the source frequency, 100 Hz; the array center is situated at a depth of 100 m. A single source is located at a range of 20 Km and a depth of 1200 m; it is assumed that there are L=11 dominant ray paths between source and array. The 11 multipath signals were pairwise 95% correlated and each was attenuated in accordance with three factors: bottom losses, attenuation proportional to path length, and cylindrical spreading factor [2]. The amplitude of each multipath arrival was selected so that the sum of the square-amplitude of each multipath arrival is equal to what it would be if the multipath signals arrived with equal strength having an SNR of 0 dB per element. The wavefront associated with each multipath arrival is modeled as being planar across the face of the array. Finally, the noise was modeled as being independent from sensor to sensor and of equal power. This simulation scenario is similar to that employed by Krolik, Lynch, and Swingler in [1] except that in their case the array was horizontally oriented and the multipath arrivals were of equal strength with 0 dB SNR per element.

Figure 1 compares the performance of the Full-coherent, "Incoherent", and Semi-coherent versions of MVDR MFP in the simulated ocean, source, and array environment described above. (Thus, any simplification or deficiency in the simulation scenario was common to the data supplied to all three algorithms.) Note that peak heights are in units of dB and are relative to the lowest point on the surface being 0 dB. For both the no mismatch and mismatch cases, the same sample covariance matrix formed from 250 snapshots was used for each of the three versions of MVDR MFP. In the mismatch case each version of MVDR MFP operated under the assumption that the ocean depth was 4500 m when it was in fact 4498 m.

Three main conclusions may be drawn from the simulation results: First, Full-coherent MVDR MFP is extremely sensitive to mismatch. A 2 m error in the assumed ocean depth caused roughly a 15 dB drop in the peak of the Full-coherent MVDR MFP ambiguity surface. Second, the performance of "Incoherent" MVDR MFP is substantially degraded relative to that of Full-coherent MVDR MFP in the no mismatch case. The peak of the "Incoherent" MVDR MFP ambiguity surface with no mismatch is roughly 15 dB less than that of the corresponding Full-coherent MVDR MFP ambiguity surface. Third, the performance of Semi-coherent MVDR MFP is both relatively robust to mismatch, with respect to error in the assumed ocean depth, and comparable in performance to Full-coherent MVDR MFP under no mismatch conditions.

These observations may be explained by examining the extent of changes in the signal arrival parameters when the ocean floor is raised by 2 m. Note that this causes a negligible change in the arrival angles of and the relative attenuations amongst the 11 multipath signals. In contrast, since 2 m is a significant fraction of the wavelength, 15 m, the relative phases amongst the 11 multipath arrivals change dramatically. This extent to which the phase of a given path changes depends on the number of bottom (B) bounces (and/or top (T) bounces) incurred en route from source to array. For example, the 2 m change in ocean depth causes a 34.5° change in the phase of the single bottom bounce path B while causing a 227.2° change in the phase of the triple bottom bounce path BTBTBT.

Full-coherent MVDR MFP assumes complete and perfect knowledge of the emitter steering vector, which is a linear combination of the path steering vectors. The path steering vectors are relatively unchanged when the ocean floor is raised by 2 m. However, the path combining coefficients, which depend on the relative phases amongst the multipath arrivals, change dramatically causing a catastrophic loss in the performance of Full-coherent MVDR MFP.

Interestingly, comparing Figures 1(c) and 1(d), it is observed that "Incoherent" MVDR MFP yielded enhanced performance in the mismatched case when the ocean floor was raised by 2 m. Although this seems counter-intuitive at first, note that in the single source case the signal-only (noise-free) output of the beam formed with the "Incoherent" MVDR weight vector is the direct sum of each multipath signal as measured at the array center. Fortuitously for "Incoherent" MVDR MFP, it turns out that for these parameters, this vector sum was larger when the ocean floor was at 4498 m then at 4500 m. In a sense, with the ocean floor at 4498 m the multipath signals were more "in-phase" than they are with the ocean floor at 4500 m. This demonstrates the strong dependence of "Incoherent" MVDR MFP on the relative phases amongst the multipath arrivals.

References

[1] J. Krolik, J. Lynch, and D. Swingler, "A Robust Incoherent Matched Field Processor for Source Localization in Uncertain Multipath Fields," *Proc. of 1989 IEEE ICASSP, May 1989, pp. 2637-2640.*

[2] W. S. Burdic, **Underwater Acoustic System Analysis**, Prentice-Hall, Englewood Cliffs, NJ, 1984.

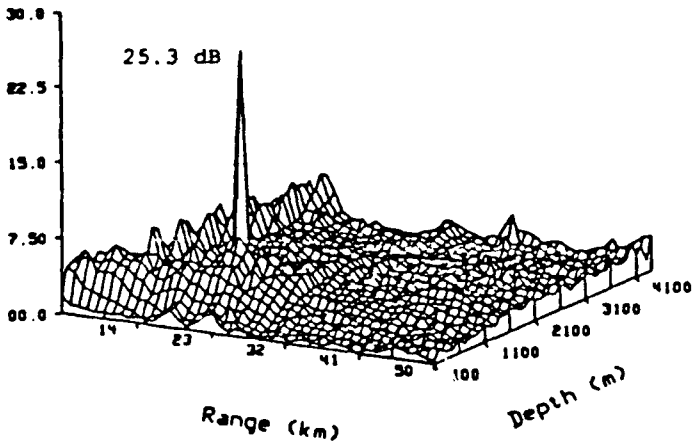

(a) Full-coherent MVDR MFP: no mismatch

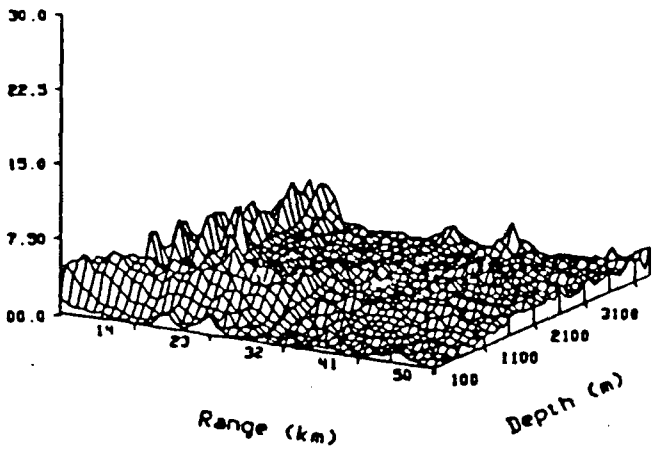

(b) Full-coherent MVDR MFP: mismatch

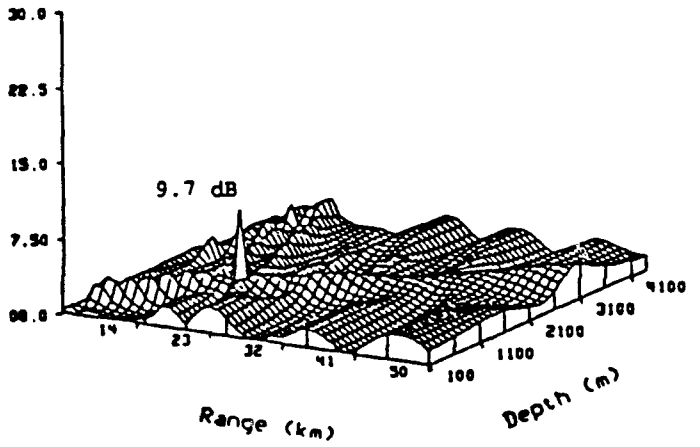

(c) "Incoherent" MVDR MFP: no mismatch

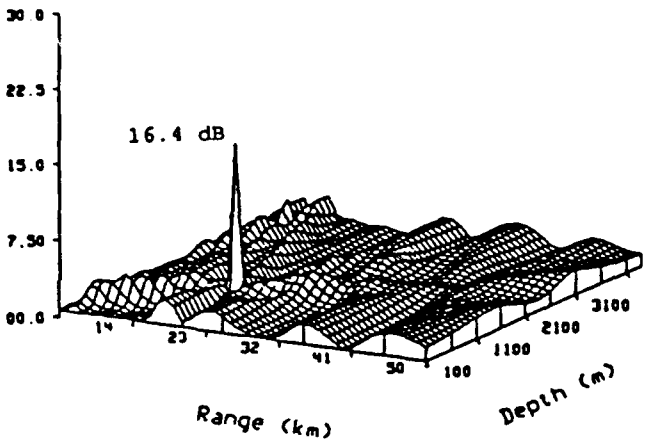

(d) "Incoherent" MVDR MFP: mismatch

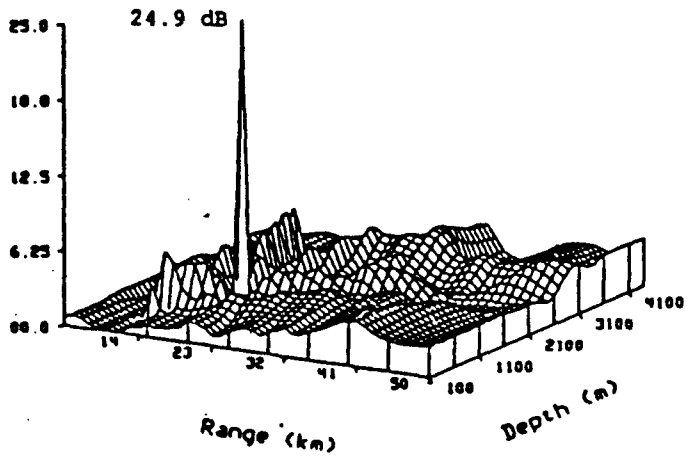

(e) Semi-coherent MVDR MFP: no mismatch

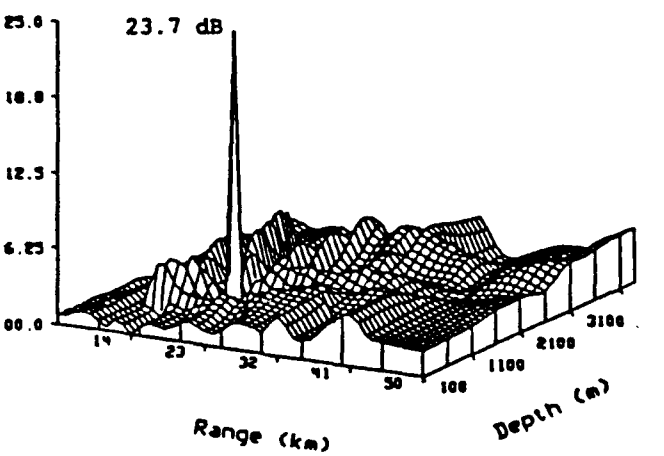

(f) Semi-coherent MVDR MFP: mismatch

Figure 1. Ambiguity surfaces generated via the Full-Coherent, "Incoherent" and Semi-coherent versions of MVDR MFP